Engineering Structures 31 (2009) 507–516

Contents lists available at ScienceDirect

Engineering Structures

journal homepage: www.elsevier.com/locate/engstruct

Component tests of buckling-restrained braces with unconstrained length

Young K. Ju [a,*,1], Myeong-Han Kim [b], Jinkoo Kim [c], Sang-Dae Kim [a]

[a] *Department of Civil, Environmental and Architectural Engineering, Korea University, South Korea*

[b] *Department of Architectural Engineering, Daejin University, South Korea*

[c] *Department of Architectural Engineering, Sungkyunkwan University, South Korea*

ARTICLE INFO

Article history:
Received 6 August 2007
Received in revised form
8 September 2008
Accepted 9 September 2008
Available online 12 November 2008

Keywords:
Buckling-restrained braces
Component test
Unconstrained length
Energy dissipation

ABSTRACT

The load-resisting capacity of buckling-restrained braces (BRB) composed of an H-shaped core element and an external tube was investigated in this study by component testing. A study was carried out on the effect of the design parameters such as the thickness of the constraining tube and the length of the unconstrained length of the core ends on the maximum strength and the energy dissipation capability. The performance of the BRB was evaluated by comparing the test results with the recommended provisions for BRB. It was found that the thickness of the external tube and the unconstrained part of the core had a significant effect on the strength and hysteretic behavior of the BRB; with the correct thickness of external tube and unconstrained length, the BRB behaved stably throughout the cyclic loading history until the cumulative plastic deformation reached 330, which far exceeded the value of 200 required by the recommended provisions.

1. Introduction

A buckling-restrained brace (BRB) generally comprises a steel core element that carries the entire axial load and a restraining exterior element that prevents the core from buckling in compression. Due to the confining effect of the exterior element, a BRB yields in both tension and compression and dissipates a significant amount of hysteretic energy during earthquakes.

The BRB has been applied in many building structures throughout the world as an economic method for seismic load-resisting systems. The seismic load-resisting capacity of BRB has been proven by numerous component and subassembly tests: Watanabe et al. [1] showed the effectiveness of buckling-restrained braces and investigated the effect of the outer tube configuration on the overall load capacity of the brace. Tremblay et al. [2] conducted a quasi-static loading test on BRB and showed that the strain hardening behavior is most likely the result of the Poisson effect on the steel plate undergoing large inelastic deformation. Huang et al. [3] carried out static and dynamic loading tests on structures with BRB and showed that the energy dissipation capacity of a frame increased with the installation of BRB, and that the main frame remained elastic even when it was subjected to large earthquake load. Black et al. [4] carried out a stability analysis against flexural and torsional buckling of BRB, and presented test results of five buckling-restrained braces with various configurations. Their study concluded that BRB is a reliable and practical alternative to conventional lateral load resisting systems.

In this study, component tests of seven buckling-restrained braces were performed to examine their behavior under simulated seismic loading. H-shaped steel sections with a constant cross-sectional area were used as core members, which were confined by an external rectangular tube that was not filled with concrete. A total of seven specimens were prepared with design variables such as the thickness of the external tube, the end reinforcement of the core, and the length of the unrestrained part of the core. The specimens were tested with loading protocol recommended by the AISC [5] to investigate the seismic capacity. Based on the test results, an investigation was carried out on the effect of the thickness of the external tube and the unrestrained length of the core on the hysteretic behavior, the failure mode, and the energy dissipation capacity.

2. Test schedule

The buckling-restrained braces investigated in this study comprise an H-shaped core element and an external tube, as shown in Fig. 1. To reduce the cost of manufacturing, the tube is not filled with any filler material (such as mortar), and the cross-sectional area of the core is kept constant. The dimensions and

* Corresponding address: Department of Civil, Environmental and Architectural Engineering, Korea University, 1, 5Ga, Anam, Sungbuk, Seoul, 136-701, South Korea. Tel.: +82 2 3290 3327; fax: +82 2 921 2439.

E-mail address: tallsite@korea.ac.kr (Y.K. Ju).

1 Previous Research Scholar, Department of Architectural, Civil, and Environmental Engineering, The University of Texas at Austin, United States.

0141-0296/$ – see front matter
doi:10.1016/j.engstruct.2008.09.014

Table 1
Size of test specimens.

No	Specimens	Core	External tube	Unconstrained length (mm)
1	B1-O-O		–	–
2	B2-R3A-L2		□ − 108 × 108 × 3t	200 (No end reinforcement)
3	B3-R4A-L2		□ − 110 × 110 × 4t	200 (No end reinforcement)
4	B4-R4B-L2	H-100 × 100 × 6 × 8(SS400)	□ − 110 × 110 × 4t	200 (End reinforcement)
5	B5-R5B-L2		□ − 112 × 112 × 5t	200 (End reinforcement)
6	B6-R4B-L3		□ − 110 × 110 × 4t	300 (End reinforcement)
7	B7-R5B-L3		□ − 112 × 112 × 5t	300 (End reinforcement)

B1: Brace specimen number 1; R3: With tube of $t = 3$ mm, O: W/O tube; A: W/O core-end reinforcement, B: With core-end reinforcement; L2: Unconstrained length = 200 mm, L3: Unconstrained length = 300 mm.

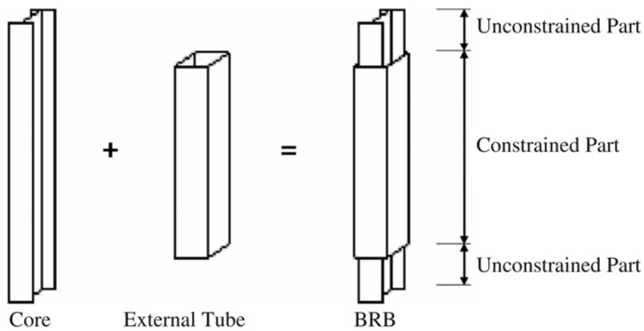

Fig. 1. The buckling-restrained brace used in the experiment.

Table 2
Results of coupon tests (MPa).

	Yield stress	Ultimate strength	Yielding ratio
Tube PL-3T	3.36	4.51	0.75
Tube PL-4T	3.53	5.01	0.70
Tube PL-5T	3.35	4.65	0.72
Core Web-6T	3.60	4.94	0.73
Core Flange-8T	3.35	4.77	0.70

detailed descriptions of the test specimens are presented in Table 1 and Fig. 2. All specimens are fabricated of SS400 steel with yield strength of 240 MPa. H-100 × 100 × 6 × 8 sections of 2.5 m length are used for core members in all specimens. The end condition of the braces is considered as a hinge. Specimen B1 is a normal steel brace not restrained by the external tube. The external tubes have three different thicknesses of 3 mm, 4 mm, and 5 mm. The core element is divided into two parts: the part constrained by the external tube and the unconstrained part which is required to make connections. The unconstrained length of specimens B2 to B5 is 200 mm and that of specimens B6 and B7 is 300 mm. The unconstrained parts of specimens B4 to B7 are reinforced with welded steel plates. 40 mm-thick plates were welded at both ends of the specimens to uniformly distribute the axial load.

The test specimens were manufactured in the order of: reinforcement of the unconstrained part of the core by welding steel plates, attachment of strain gages, placement of the core inside the external tube, and reinforcement of the ends of the external tube. To prevent excessive slip between the core and the tube, stoppers were welded at the flange of the core. Figs. 3 and 4 show the process of manufacturing the specimens and the locations of the strain gages, respectively. Fig. 5 shows the test setup for the component test of BRB. The experiments were carried out using a universal testing machine with a maximum capacity of 3000 kN. To evenly distribute the axial load along the cross-section, a 40 mm-thick steel plate and a pin-zig were tightly connected by high-tension bolts at the ends of the brace. The axial deformation of the test specimens was measured by a load-cell and two LVDT's. The applied loading histories (the Loading Protocol 2 of the Recommended Provision [5] shown in Fig. 6), included a quasi-static cyclic test with stepwise incremental displacement amplitudes at a constant rate of 0.01 mm/s [6,7]. To assess the maximum cumulative plastic deformation and energy-dissipation capacity, the load was increased until the maximum displacement of $2.0D_{bm}$ (the maximum displacement regulated by the loading protocol), was exceeded and failure occurred [8].

To evaluate the mechanical properties of the structural steel of the BRBs, a coupon test was carried out in accordance with the Korean Standard KSB 0801. 3 mm, 4 mm, and 5 mm thick coupons were taken out of the flange and the web of the core member and of the external tube. The test specimens were fabricated of mild steel SS400 with nominal yield stress of 240 MPa. The tensile test results are summarized in Table 2, where it can be seen that all the specimens satisfied the requirements of the Korean Standard.

3. Results and analysis

3.1. Failure modes

From the experiments, it was observed that the specimens failed either by flexural buckling at the end of the core or by

Table 3
Ultimate strength and failure mode of test specimens.

Specimens	Point of buckling	P_{max} (kN)	Failure mode	Observation
B1-0-0	1-1	30.20	Global buckling in the middle of the specimen	Buckling at the computed critical load (31.6 kN)
B2-R3A-L2	2-1	49.79	Flexural yielding of tube before compressive yielding of core	Lack of bending strength of external tube
B3-R4A-L2	2-1	58.36	Flexural yielding of core-end before yielding of core	Lack of bending strength of core-end
B4-R4B-L2	2-1	66.64	Flexural yielding of tube before compressive yielding of core	Lack of bending strength of external tube
B5-R5B-L2	4-1	76.80	Flexural yielding of tube followed by compressive yielding of core	Inelastic deformation, slight lack of bending strength of tube
B6-R4B-L3	3-1	71.40	Flexural yielding of tube followed by compressive yielding of core	Inelastic deformation, slight lack of bending strength of tube
B7-R5B-L3	7-1	86.80	Compressive yielding of core followed by flexural yielding of tube	Inelastic deformation, satisfaction of AISC requirements

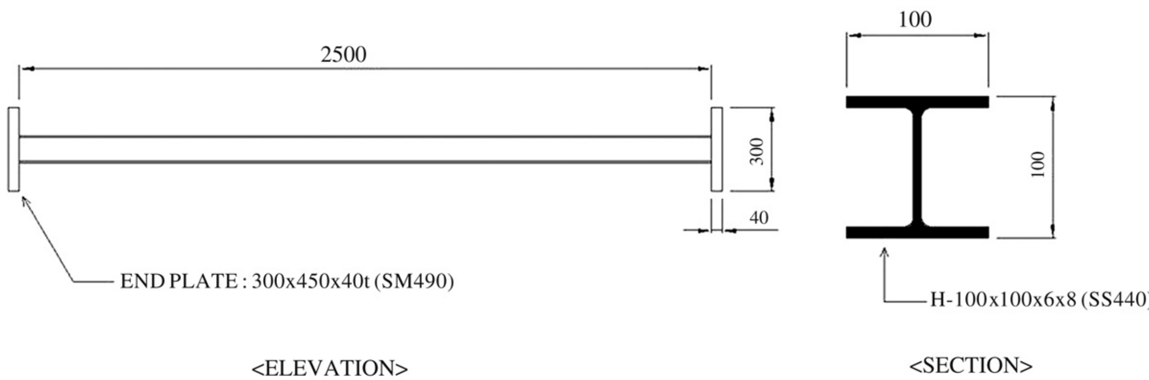

(a) Specimen B1-0-0.

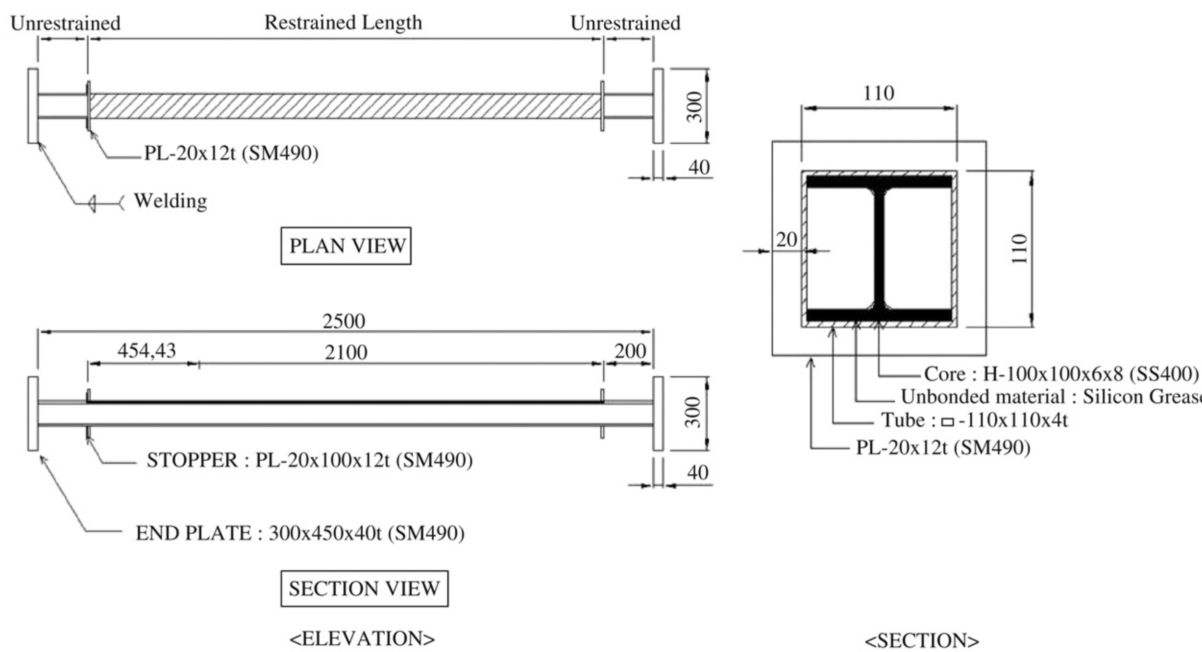

(b) Specimen B3-SR3A-L2.

Fig. 2. Details of the test specimens.

flexural yield in the middle of the external tube. The ultimate strength and the failure mode of test specimens are summarized in Table 3. The load–displacement relationship and the failure modes are also depicted in Figs. 7 and 8, respectively. It can be observed that the specimen not restrained by an external tube (B0-0-0) failed by buckling at the first compressive loading cycle. However, specimen B7, which had the thickest external tube and a 300 mm unconstrained length with reinforcement, showed superior performance to the other specimens, while displaying stable hysteretic curves until the ductility ratio reached 15. The test results showed that the maximum strength increases as the unconstrained length of the core increases to 300 mm and as the thickness of the external tube increases. Furthermore, the addition of the stiffener which shortens the core length also plays a role.

3.2. Effect of the design parameters

Fig. 9 shows a comparison of the load–displacement relationship of the specimens at their maximum compressive loading cycle. It can be observed that the specimens with a 5 mm-thick external tube (B5 and B7) showed superior performance in maximum displacement as well as strength. In particular, the maximum deformation of specimen B7, with 300 mm unconstrained length, is more than twice that of specimen B5 with 200 mm unconstrained length.

Fig. 10 shows the load–displacement relationship of specimens with various thicknesses of external tube. When the unconstrained length is 200 mm, the maximum compressive strengths of specimens with tube thickness of 4 mm and 5 mm are 34% to 54% larger, respectively, than that of the specimen with 3 mm tube thickness. This can be expected because the increase in thickness causes an increase in the bending stiffness and strength of the external tube, which results in an increase in the axial-load resisting capacity of the core elements. For economy, however, the thickness of the external tube needs to be optimized.

To find the effect of the constrained length at the end of the core, the B4-R4B-L2 specimen was tested under the same loading condition as that of the B3-R4A-L2 specimen. The inelastic deformation is planned to start at the second cyclic loading stage, which is $0.5D_{bm}$ (=7.15 mm). The strains of the B4-R4B-L2 specimen, measured in the longitudinal direction at the first cyclic load at the second loading stage are shown in Fig. 11, where the

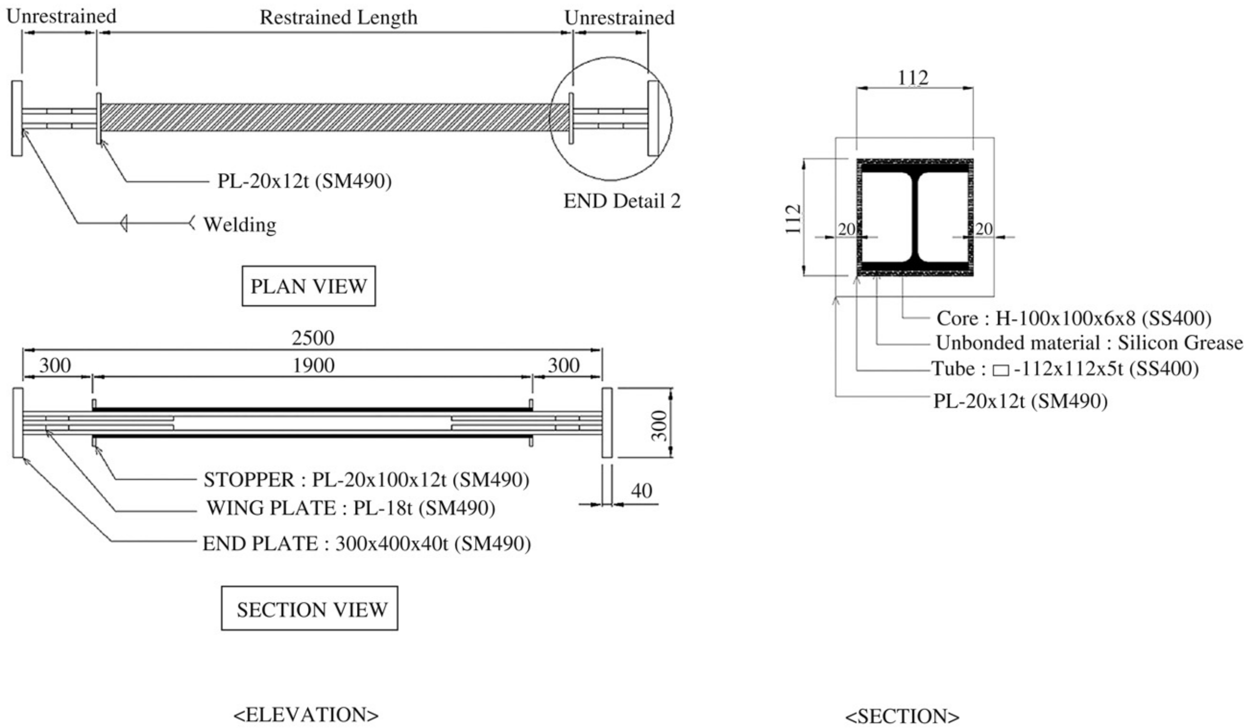

(c) Specimen B7-SR3A-L3.

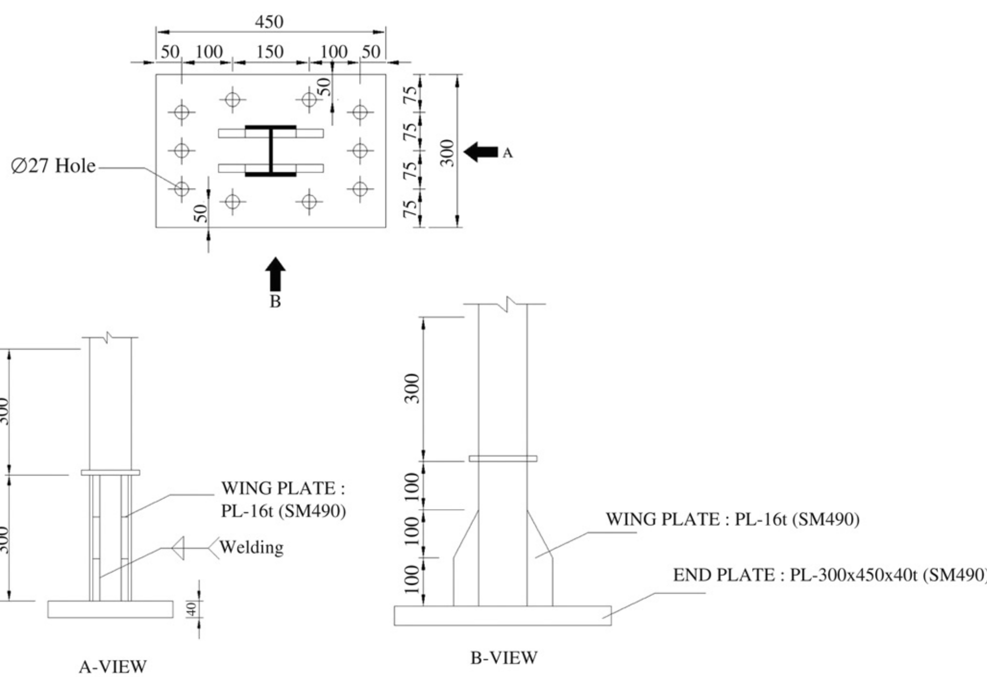

(d) End details.

Fig. 2. (*continued*)

measuring locations are at the center of the core and tube, and at the end of the core.

In the case of specimen B3-R4A-L2 with an unconstrained length at both ends, the flexural deformation in the weak axis was found at the end of the core accompanying the degradation of the strength. The flexural deformation of the core at the end is determined by the combination of the axial force of the core and the bending moment due to out-of-plane deformation. For the BRB that had an unconstrained length of over 200 mm at the end of the core, the increased section is recommended at the end of the core in order to obtain the required compressive strength.

The effect of unconstrained length is plotted in Fig. 12, where a comparison is shown of the load–displacement curves of four specimens at maximum compression. It can be observed that the maximum strengths of the specimens with an unconstrained length of 300 mm (B6 and B7) are 8%–13% larger than those of

(a) Welding of the core-end with end plate.

(b) Welding of cover plate for reinforcement.

(c) Attachment of strain gages.

(d) Reinforcement of tube end.

Fig. 3. Manufacturing of the buckling-restrained braces used in the experiments.

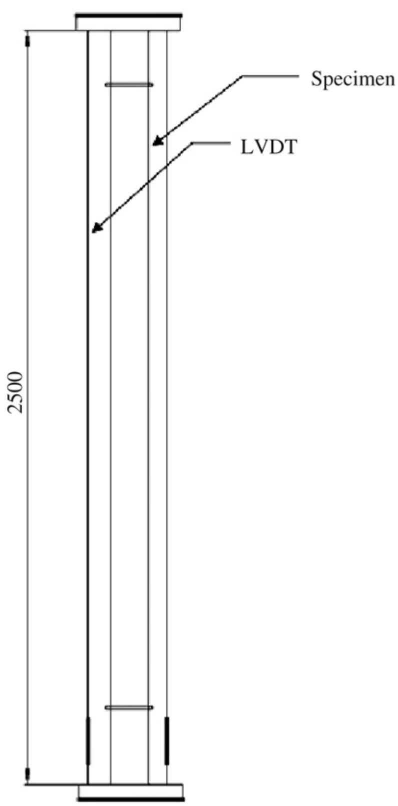

(a) Elevation.

(b) Sections.

Fig. 4. Location of LVDT's and strain gages.